

Carbon nanotube films change Poisson's ratios from negative to positive

Yin Ji Ma,¹ Xue Feng Yao,^{1,a)} Quan Shui Zheng,^{1,a)} Ya Jun Yin,¹ Dong Jie Jiang,¹
Guang Hui Xu,² Fei Wei,² and Qiang Zhang²

¹Department of Engineering Mechanics, Applied Mechanics Laboratory, Tsinghua University,
Beijing 100084, People's Republic of China

²Department of Chemical Engineering, Beijing Key Laboratory of Green Chemical Reaction Engineering
and Technology, Tsinghua University, Beijing 100084, People's Republic of China

(Received 7 May 2010; accepted 16 July 2010; published online 11 August 2010)

In this paper, a discovery is reported that carbon nanotube (CNT) films can change in-plane Poisson's ratios from negative to positive during a uniaxial tensile loading. First, *in situ* experimental investigations of the deformation fields about the CNT films fabricated using vertically aligned CNT arrays are performed by digital speckle correlation method, the novel phenomenon for changing Poisson's ratio from negative to positive during the stretching process is discovered. Furthermore, the physical mechanisms for changing the Poisson's ratio from negative to positive are explained based on the interactions among CNTs. Finally, a potential engineering application for designing intelligent connector is proposed based on the intriguing Poisson's ratio of CNT films.
© 2010 American Institute of Physics. [doi:10.1063/1.3479393]

Usually solid materials under axial load experience lateral contraction with a positive Poisson's ratio. The Poisson's ratio equals to 0.5 if the volume of the material does not change during the stretching process. In fact, most solid materials increase their volumes slightly when being stretched and have Poisson's ratios about 0.3. Recently, advanced materials (auxetic materials¹) with negative Poisson's ratio such as foams,^{2,3} honeycombs⁴ and carbon nanotube (CNT) material,⁵ have been investigated by many researchers due to their special functions and engineering applications. CNTs have extraordinarily high tensile strength and Young's modulus, and CNT films show amazing mechanical properties. Hall *et al.*⁵ found CNT sheets with negative Poisson's ratios and established a theoretical model to explain the physical mechanism. Chen *et al.*⁶ investigated the negative Poisson's ratios in different directions of highly oriented CNT films. However, the change in Poisson's ratio from negative to positive with the increasing of the applied strain was few reported. In this paper, *in situ* experimental investigations of positive and negative Poisson's ratio for the CNT films were performed to reveal the intriguing Poisson's ratio transition.

Vertically aligned CNTs (VACNTs) with an aspect ratio of over 10^4 were selected as building blocks to fabricate CNT films via a facile dispersion-filtration method.⁷ Two kinds of VACNT arrays with different CNT outer diameters were adopted: (i) 30-nm-CNTs with a length of 5.0 mm and a diameter of 30–60 nm, which were fabricated by a floating catalyst chemical vapor deposition (CVD)⁸ [Fig. 1(a)]; (ii) 10-nm-CNTs with a length of 0.2 mm and a diameter of 8–12 nm, which were fabricated by a thermal CVD method.⁹ Both VACNT arrays were directly used without any specific purification and dispersed by a two-step shearing method.^{10,11} As-obtained CNT dispersions were filtrated to fabricate CNT films.⁷ When the filtration stopped, the CNT films can be easily separated from the microporous filter

membrane. Figure 1(b) shows a macroscopic photo of the CNT film. Figures 1(d) and 1(e) show the scanning electronic microscope (SEM, JSM 7401F operating at 3.0 kV) micrographs of films about 10-nm-CNTs and 30-nm-CNTs, respectively.

Tensile fracture experiments on two kinds of CNT films were performed using electronic universal testing machine (WD-4020). The deformation fields of the CNT film were obtained using digital speckle correlation method.^{12–15} The tensile deformation speckle image for 10-nm-CNT film is shown in Fig. 2(a). Here, X and Y are the directions which are parallel and perpendicular to direction of the applied tensile loading, respectively. Both U and V fields are the incremental displacement fields of CNT films in X and Y directions, respectively. When the stress increased from 2.7 to 3.5 MPa, both U and V fields of 10-nm-CNT film were positive [Figs. 2(b) and 2(c)]. It indicated that when the CNTs film was elongated in X direction, it expanded in Y direction.

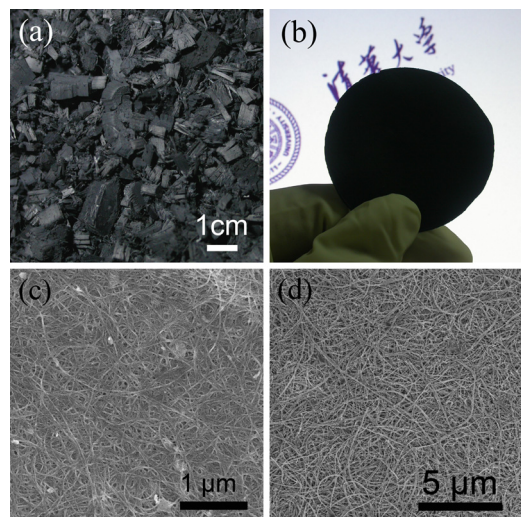


FIG. 1. (Color online) [(a) and (b)] Macrographs of the VACNTs and the CNT film. [(c) and (d)] SEM micrographs of 10-nm-CNT and 30-nm-CNT films.

^{a)}Authors to whom correspondence should be addressed. Electronic addresses: yxf@mail.tsinghua.edu.cn and zhengqs@tsinghua.edu.cn. Tel.: +86-10-62771546 and +86-10-62771112. FAX: +86-10-62781824 and +86-10-62771113.

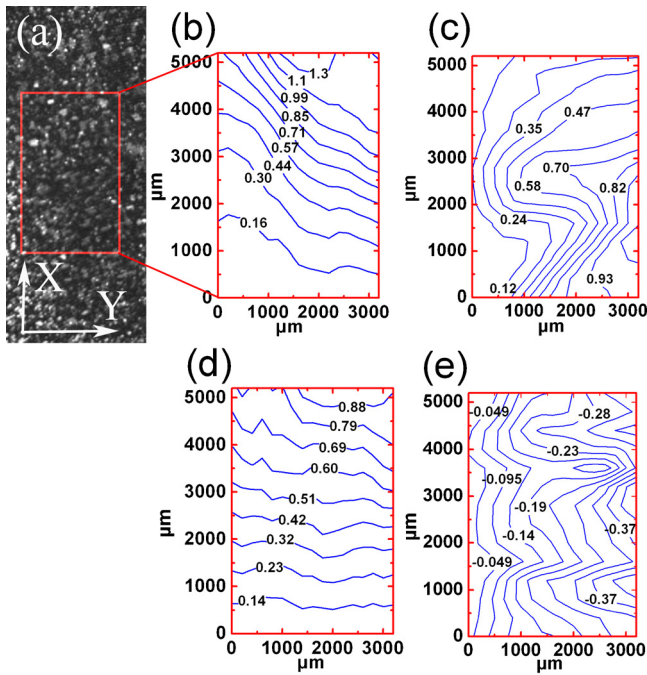


FIG. 2. (Color online) Displacement field of 10-nm-CNTs film (a) calculated zone. [(b) and (c)] the incremental displacement fields in the Y- and X-directions loading from 2.7 to 3.5 MPa. [(d) and (e)] those from 8.8 to 9.7 MPa.

When the stress increased from 8.8 to 9.9 MPa, both U and V fields of 10-nm-CNT film were positive and negative [Figs. 2(d) and 2(e)], respectively. It indicated that the CNTs film shrank in Y direction during its elongation.

Figure 3(a) shows the relationship between the variation in length and width for 10-nm-CNT film and 30-nm-CNT film, respectively. L_0 and W_0 were defined as the length and the width of the CNT films before tensile test, respectively. ΔL and ΔW were the increment of the length and the width, respectively. When $\Delta L/L_0$ was small, the $\Delta W/W_0$ increased with $\Delta L/L_0$ increasing. However, when $\Delta L/L_0$ increased to a certain amount, $\Delta W/W_0$ decreased.

Based on both U and V fields, the in-plane Poisson's ratio of the CNT-film can be obtained. Here, the instantaneous in-plane Poisson's ratio was defined as

$$\nu = - \frac{d\varepsilon_Y/d\sigma}{d\varepsilon_X/d\sigma},$$

where ε_Y and ε_X are the strain in the Y and X directions, respectively, σ is the stress in the X direction. Figure 3(b) showed the relationship between the in-plane Poisson's ratio and the strain of 10-nm-CNT film and 30-nm-CNT film, respectively. When ε_X was small ($<0.8\%$ for 10-nm-CNT film and $<0.4\%$ for 30-nm-CNT film, respectively), the in-plane Poisson's ratio was negative. With the increased strain, the in-plane Poisson's ratio also increased and became positive gradually.

The evolution mechanism of the Poisson's ratio can be interpreted simply by means of two-dimensional (2D) schematic illustration (Fig. 4). Figure 4(a) illustrated the status of the CNT films under tension. Each line in Fig. 4(a) represented an individual CNT. At the early stage, the CNTs in the film were bended, and then they tended to be straightened gradually. The evolution of the basic unit structure was simulated as shown in Fig. 4(c) using ABAQUS software which

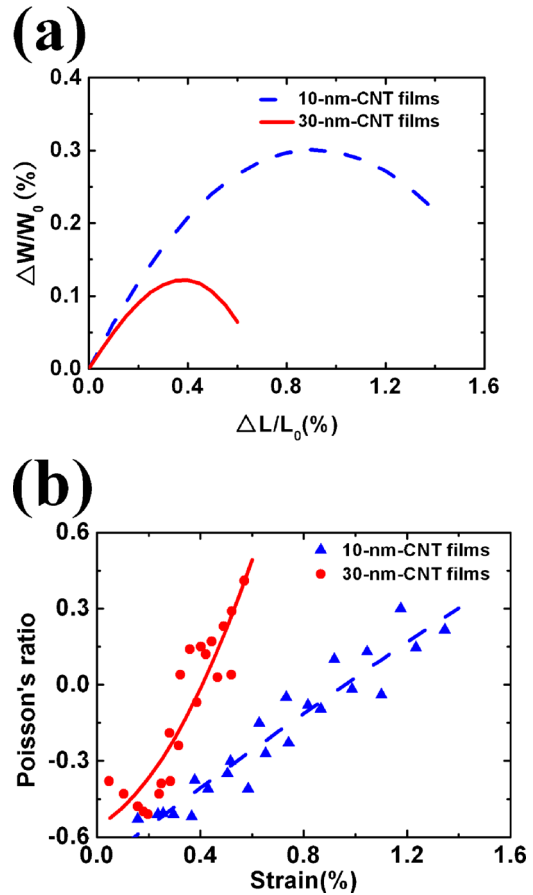


FIG. 3. (Color online) The results of tensile fracture experiments: (a) the relationship between the length and the width of CNT films. (b) The relationship between the Poisson's ratio and the strain of CNT films.

is a commercial software package for finite element analysis developed by HKS Inc. of Rhode Island, USA. From the SEM micrographs of 10-nm-CNT and 30-nm-CNT films [Figs. 1(c) and 1(d)], the structures of the CNT films are very complicated and the meandering CNTs in CNT film are pliable. The energy increment for elongating specimens is mainly absorbed by the straightened CNTs. Thus the sample

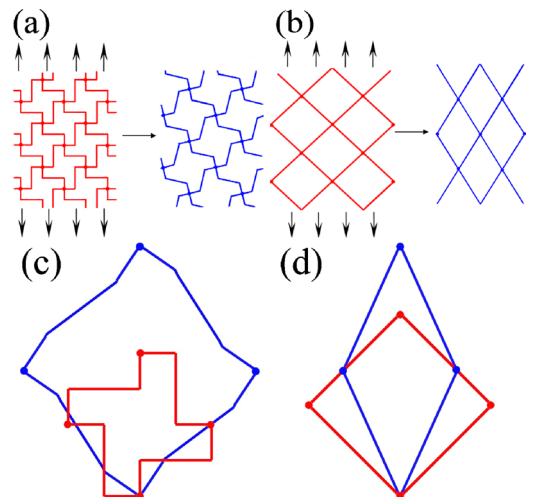


FIG. 4. (Color online) Deformation mechanisms: [(a) and (b)] deformation mechanisms of CNTs film for negative and positive Poisson's ratios. [(c) and (d)] The evolutions of the basic unit structure for negative and positive Poisson's ratios.

expanded laterally and the in-plane Poisson's ratio was negative. When the strain increased to a certain level, the CNTs tended to be straightened gradually. Until most of CNTs were straightened [Fig. 4(b)], the effective tensile stiffness of the isolated CNT increased. Thus, the angle between the CNTs was changed at this time to absorb the energy increment for the elongating specimens. During the stretching process, the Poisson's ratio changed from negative to positive.

A three-dimensional (3D) model has been developed to predict the in-plane Poisson's ratio of the CNT film by Hall *et al.*^{5,16} The in-plane Poisson's ratio is given by $\nu = (1 - \beta) / (3 + \beta)$,⁵ where $\beta = 3K_T / K_{SB}$, K_T is the torsional material constant which represents internanotube junction stiffness, K_{SB} is the combination of the stretching material constant and the bending material constant which represents the effective tensile stiffness of the isolated CNT. This 3D model is used to explain the phenomenon of changing Poisson's ratio. It indicates that the Poisson's ratio ν approximately equals to -1 when the CNTs are very pliable ($K_{SB} \rightarrow 0, \beta \rightarrow \infty$). In 2D schematic illustration, the CNTs were pliable at the beginning of loading, the effective tensile stiffness K_{SB} was small and β was large, thus a negative Poisson's ratio was formed [Fig. 3(b)]. With the increase in the applied strain, the CNTs became more rigid. If the CNTs are rigid ($K_{SB} \rightarrow \infty, \beta \rightarrow 0$), the Poisson's ratio ν is close to $1/3$ according to the 3D model. In 2D schematic illustration, when the CNTs were straightened gradually, the effective tensile stiffness of an isolated CNT increased and the Poisson's ratio became positive gradually [Fig. 3(b)]. Two explanations agreed well with each other as well as with the experimental observation of the Poisson's ratio.

In summary, the in-plane Poisson's ratios of CNT films were *in situ* investigated using digital speckle correlation method, which changed from negative to positive during the stretching process. The physical mechanisms of the positive and negative in-plane Poisson's ratio are explained which agreed well with the experimental observation. The negative Poisson's ratio lies in the elongation of bending CNTs, and the positive Poisson's ratio lies in the angle variation between CNTs. The material with such a variation in Poisson's

ratio has a potential engineering application. For example, a connector is designed to connect two other devices depending on friction. The lateral dimension of the connector will expand while increasing the tension, then the friction will increase and it will not easy to fall off. But when the tension increases to a certain amount, the lateral dimension of the connector will shrink, and then the tension decreased while increasing the friction. The maximum tension is limited for the connector.

This project was supported by China Science and Technology 863 project (Grant No. 2008AA03Z302), the Natural Scientific Foundation of China (Grant Nos. 20736004, 20736007, and 2007AA03Z346) and the China National Program (Grant No. 2006CB932702).

¹R. Lakes, *Science* **235**, 1038 (1987).

²J. B. Choi and R. S. Lakes, *Int. J. Fract.* **80**, 73 (1996).

³J. N. Grima, R. Gatt, N. Ravirala, A. Alderson, and K. E. Evans, *Mater. Sci. Eng., A* **423**, 214 (2006).

⁴M. R. Hassan, F. Scarpa, and N. A. Mohamed, *J. Intell. Mater. Syst. Struct.* **20**, 897 (2009).

⁵L. J. Hall, V. R. Coluci, D. S. Galvao, M. E. Kozlov, M. Zhang, S. O. Dantas, and R. H. Baughman, *Science* **320**, 504 (2008).

⁶L. Z. Chen, C. H. Liu, J. P. Wang, W. Zhang, C. H. Hu, and S. S. Fan, *Appl. Phys. Lett.* **94**, 253111 (2009).

⁷G. H. Xu, Q. Zhang, W. P. Zhou, J. Q. Huang, and F. Wei, *Appl. Phys. A: Mater. Sci. Process.* **92**, 531 (2008).

⁸Q. Zhang, J. Q. Huang, M. Q. Zhao, W. Z. Qian, Y. Wang, and F. Wei, *Carbon* **46**, 1152 (2008).

⁹X. B. Zhang, K. L. Jiang, C. Teng, P. Liu, L. Zhang, J. Kong, T. H. Zhang, Q. Q. Li, and S. S. Fan, *Adv. Mater.* **18**, 1505 (2006).

¹⁰Q. Zhang, G. H. Xu, J. Q. Huang, W. P. Zhou, M. Q. Zhao, Y. Wang, W. Z. Qian, and F. Wei, *Carbon* **47**, 538 (2009).

¹¹G. H. Xu, Q. Zhang, J. Q. Huang, M. Q. Zhao, W. P. Zhou, and F. Wei, *Langmuir* **26**, 2798 (2010).

¹²G. C. Jin, Z. Wu, N. K. Bao, and X. F. Yao, *Opt. Lasers Eng.* **39**, 457 (2003).

¹³X. F. Yao, L. B. Meng, J. C. Jin, and H. Y. Yeh, *Polym. Test.* **24**, 245 (2005).

¹⁴L. B. Meng, G. C. Jin, and X. F. Yao, *Opt. Lasers Eng.* **45**, 57 (2007).

¹⁵X. F. Yao, P. Wang, and R. C. Dai, *J. Biomed. Opt.* **13**, 034026 (2008).

¹⁶V. R. Coluci, L. J. Hall, M. E. Kozlov, M. Zhang, S. O. Dantas, D. S. Galvao, and R. H. Baughman, *Phys. Rev. B* **78**, 115408 (2008).